

Pressure-induced phase transition of SiC

Murat Durandurdu

Department of Materials Science and Engineering, University of Michigan, Ann Arbor,
MI 48109, USA

Received 24 April 2003

Published 11 June 2004

Online at stacks.iop.org/JPhysCM/16/4411

doi:10.1088/0953-8984/16/25/002

Abstract

The pressure-induced phase transition in silicon carbide is studied using a constant-pressure *ab initio* technique. The reversible transition between the zinc-blende structure and the rock-salt structure is successfully reproduced through the simulation. The transformation mechanism at the atomistic level is characterized, and it is found that the transition is based on a tetragonal and an orthorhombic intermediate state. The space groups of the intermediate states are determined as $I\bar{4}m2$ and $Imm2$.

1. Introduction

Silicon carbide (SiC) has outstanding physical properties, such as a wide bandgap, high stiffness, high hardness, high thermal conductivity and a high melting point, and hence it is of technological importance for electronic and optoelectronic device applications. At ambient conditions, SiC can form in many different crystallographic modifications that originate from differences in the stacking sequence of the silicon–carbon pair layers. More than 100 polytypes of SiC are known at atmospheric pressure [1].

A number of experimental and theoretical studies have been carried out to better understand the pressure-induced phase transition of SiC [2–8]. X-ray diffraction measurements [3] have shown that SiC undergoes a phase transition with a volume drop of $\sim 20.3\%$ from the zinc-blende (B3) structure to the rock-salt (B1) structure at around 100 GPa. The transition is reversible and the zinc-blende phase is recovered below 35 GPa upon decompression. Shock compression studies [4] have also found that the high-pressure phase of SiC is the rock-salt structure above 100 GPa. In the *ab initio* density-functional calculations [5, 6], the transition pressure is predicted to be a lower value of 66 GPa.

Because of the limitations of experimental information at the atomistic level, reliable dynamical simulations are desirable. Such simulations may fully describe the microscopic nature of transformation mechanisms and electronic structure of phases for each applied pressure. Recently, the phase transformation of SiC was investigated by a molecular dynamics (MD) simulation using an inter-atomic potential [7] and it was found that the transformation mechanism is associated with a cubic to monoclinic unit-cell transformation,

and Si and C sublattices shift with respect to each other along the $\{100\}$ direction in the zinc-blende structure. This observation does not agree with the simple transformation mechanism based on a rhombohedral $R3m$ intermediate state proposed in the first-principles calculation [6]. Catti [8] characterized the recent MD simulation result [7] using an *ab initio* method and proposed a new transformation pathway with an orthorhombic intermediate state having a much lower activation energy than $R3m$. The orthorhombic structure was described as having the space group of $Pmm2$ (see [8]). On the other hand, Mato *et al* [9] pointed out that the transformation mechanism proposed in [8] was established without systematic symmetry considerations, and using group theory analysis they suggested that the symmetry of the orthorhombic intermediate state should be corrected to $Imm2$ because $Imm2$ is actually one of the maximal subgroups of the zinc-blende structure. The transition mechanism in cubic and other forms of SiC was also investigated by Miao *et al* [10–12] using an *ab initio* technique. Their results provided further substantial information on the transition pathways in SiC and, moreover, they also revealed that the intermediate phase has $Imm2$ symmetry.

The transition mechanism proposed for the zinc-blende to rock-salt structure in these studies is based on only one intermediate state. However, the transformation pathway for a reconstructive phase transition is not straightforward and the path is associated with large atomic displacements and/or strain [13]. Therefore, the system can transform from one phase to another by passing through various closely related paths during the transition [10]. In other words, the transformation mechanism might follow various transition pathways or involve several intermediate states. Actually, recent systematic group-theoretical analysis suggests several competitive low-barrier pathways for the zinc-blende to rock-salt transformation of SiC in addition to the $Imm2$ phase [14]. In this paper, we carry out an *ab initio* constant-pressure method to clarify the transformation mechanism of SiC. Our findings bring a new level of understanding of the $B3 \rightleftharpoons B1$ transition and suggest that the transition pathway does indeed involve both a tetragonal ($I\bar{4}m2$) and an orthorhombic ($Imm2$) intermediate unstable phase.

2. Methodology

We perform the first-principles pseudopotential method within the density-functional formalism and the local-density approximation using the Ceperley–Alder functional [15] for the exchange–correlation energy. The calculation is carried out with the *ab initio* program SIESTA [16] using a linear combination of atomic orbitals as the basis set, and norm-conserving Troullier–Martins pseudopotential [17]. A split-valence single- ζ basis set is employed. A uniform mesh with a plane wave cut-off of 40 Ryd is used to present the electron density, the local part of the pseudopotential, and the Hartree and the exchange–correlation potential. We use Γ -point sampling for the supercell’s Brillouin zone integration, which is reasonable for a simulation cell with 64 atoms. Pressure is applied via the method of Parrinello and Rahman [18].

In constant-pressure simulations, heterogeneous nucleation is suppressed because of the use of a perfect crystal with periodic boundary conditions, and hence large hysteric effects are observed. In order to obtain a phase transition within the accessible simulation time, a simulation box has to be superpressurized [19, 20], and therefore the transition pressures and volumes are found to be substantially different from experiments. Nevertheless, the techniques successfully reproduce high-pressure phases of materials. In the present study, we begin the simulation at a high pressure and use a large increment of 100 GPa/1000 fs in order to reduce the computational effort.

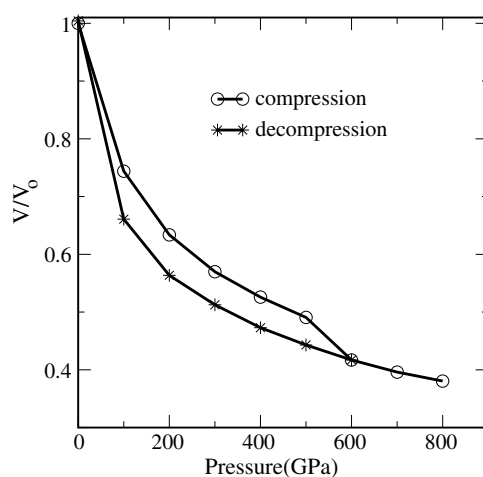


Figure 1. The pressure–volume curve of SiC on compression and decompression.

3. Results and discussion

Figure 1 shows the volume change of SiC as a function of the applied pressure. The volume decreases monotonically and the zinc-blende structure is still preserved up to 500 GPa. As the applied pressure is increased from 500 to 600 GPa, the structural transition begins and is accompanied by a dramatic volume drop of the simulation cell. At this pressure, the zinc-blende structure transforms into a rock-salt phase, in agreement with experiment [3].

Upon pressure release from the rock-salt phase at 600 GPa, we find that the structure transforms back to a zinc-blende phase between 100 and 0 GPa with a large volume jump. The reverse transition observed is also in good agreement with experiment [3]. The zinc-blende structure obtained on decompression does not have any defects, but it is slightly distorted.

The volume–pressure relations for the zinc-blende structure (0–500 GPa) and for the rock-salt structure (100–800 GPa) are fit to the third-order Birch–Murnaghan equation of state. The fitting yields the bulk modulus $K = 194.97$ GPa, and its pressure derivative $K' = 3.72$ for the zinc-blende structure. These results are consistent with experimental and theoretical data: $K = 196$ – 240 GPa and $K' = 2.9$ – 3.77 (see [3, 6]). The calculated equation of state parameters $K = 239.98$ GPa and $K' = 3.63$ for the rock-salt structure are found to be in good agreement with the theoretical values of $K = 252$ GPa and $K' = 4.26$ (see [6]).

The simulation cell lengths and angles at 600 GPa shown in figure 2 provide information regarding the structural changes at the atomistic level. The lattice structure is simultaneously compressed along the B -axis ($\{010\}$ direction) and elongated along the other axes, which leads to the onset of a phase transformation in the system. The angle β , which gives a measure of the monoclinic distortion in the structure, turns out to be 70° , whereas the other angles are invariant during the transformation. These observations indicate that the phase transition into the rock-salt structure is due to the monoclinic modification of the simulation cell as reported in the previous simulation [7]. We should note here that, before the monoclinic deformation occurs, the cubic cell first transforms into a tetragonal cell and then the tetragonal structure converts to a monoclinic one as clearly seen in figure 2. Similar behaviour, indeed, can be seen in figure 3 of the MD simulation [7], but the authors missed this point. Therefore, the cubic \rightarrow tetragonal \rightarrow monoclinic deformation should be a true mechanism for the zinc-blende to rock-salt transformation.

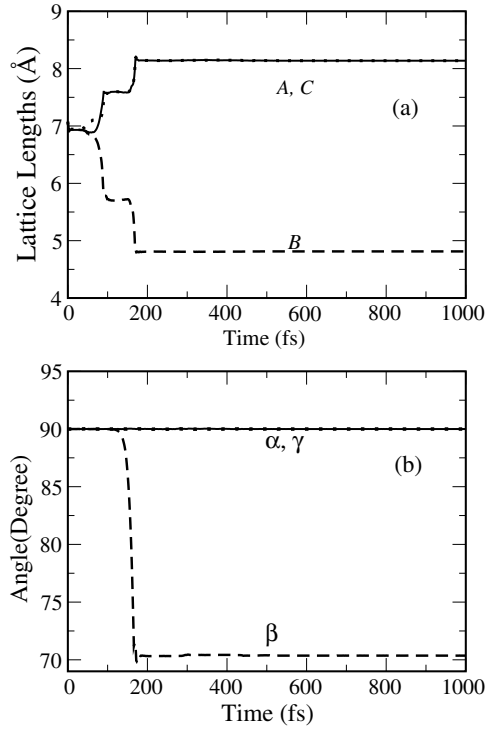


Figure 2. The time evolution of simulation cell lengths and angles at 600 GPa.

We analyse the symmetry change of the structure during the transformation using the KPLOTT program [21], which gives detailed information about space group, cell parameters and atomic positions for a given structure. The onset of symmetry breaking in the system is observed near 88 fs and at this point the cubic structure transforms to a tetragonal one with the unit-cell parameters $a = b = 2.60567 \text{ \AA}$ and $c = 3.019 \text{ \AA}$. The corresponding space group of the tetragonal phase is $I\bar{4}m2$. When the β angle is about 83° , an orthorhombic state is formed. The orthorhombic phase has $Imm2$ symmetry and is characterized by the lattice constants $a = 2.51618 \text{ \AA}$, $b = 2.85727 \text{ \AA}$ and $c = 2.8350 \text{ \AA}$. The result confirms that the intermediate orthorhombic state does indeed have $Imm2$ not $Pmm2$ symmetry. The transformation into a rock-salt structure begins as the β angle reaches a value of 75° . The lattice parameter of the rock-salt structure is found to be 3.3460 \AA , which is, however, less than the experimental value of 3.648 \AA (see [3]). The atomic positions and unit-cell parameters of both intermediate states are given in table 1. It should be noted that these parameters are also underestimated since the system was superpressurized and transformed a dense rock-salt structure.

The relations between the simulation cell (64 atoms) and the unit cells are also determined by the KPLOTT program. For the zinc-blende structure, the unit-cell vectors \mathbf{a} , \mathbf{b} and \mathbf{c} are parallel to the simulation cell vectors \mathbf{A} , \mathbf{B} and \mathbf{C} and hence $\mathbf{a} = \mathbf{A}/4$, $\mathbf{b} = \mathbf{B}/4$ and $\mathbf{c} = \mathbf{C}/4$. With the modification to tetragonal phase, the unit-cell vectors become $\mathbf{a} = -(\mathbf{A} + \mathbf{C})/4$, $\mathbf{b} = (-\mathbf{A} + \mathbf{C})/4$ and $\mathbf{c} = \mathbf{B}/2$. The same relations hold for the orthorhombic state except that the signs of \mathbf{b} and \mathbf{c} are changed. For the rock-salt structure, the unit-cell vectors can be calculated using the following relations: $\mathbf{a} = (\mathbf{A} - 2\mathbf{B} - \mathbf{C})/4$, $\mathbf{b} = (\mathbf{A} + 2\mathbf{B} - \mathbf{C})/4$ and $\mathbf{c} = (\mathbf{A} + \mathbf{B})/4$.

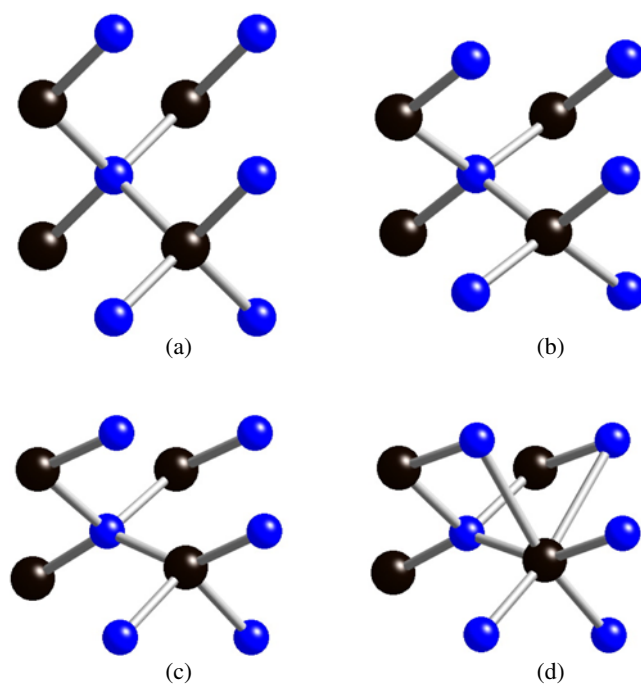


Figure 3. The evolution of the rock-salt structure at 600 GPa. (a) The zinc-blende structure at 1 fs; (b) the intermediate tetragonal phase at 88 fs; (c) the orthorhombic state at 150 fs; (d) the formation of the rock-salt structure at 160 fs.

(This figure is in colour only in the electronic version)

Table 1. The atomic positions and the lattice parameters of the observed intermediate states on loading (LD) at 600 GPa and unloading (ULD) at 0 GPa.

Phase	Lattice parameters (\AA)	Atomic positions (x, y, z)
Tetragonal $I\bar{4}m2$ (LD)	$a = 2.605\ 67$ $b = 2.605\ 67$ $c = 3.019\ 00$	C: 0.0 0.5 0.75 Si: 0.0 0.0 0.5
Orthorhombic $Imm2$ (LD)	$a = 2.516\ 18$ $b = 2.857\ 27$ $c = 2.835\ 00$	C: 0.0 0.5 0.034 207 Si: 0.0 0.0 0.221 632
Tetragonal $I\bar{4}m2$ (ULD)	$a = 3.450\ 64$ $b = 3.450\ 64$ $c = 3.657\ 75$	C: 0.0 0.0 0.0 Si: 0.0 0.5 0.75
Orthorhombic $Imm2$ (ULD)	$a = 4.099\ 60$ $b = 3.460\ 00$ $c = 2.912\ 58$	C: 0.0 0.0 0.536 372 Si: 0.0 0.5 0.174 363

A close analysis during the transformation reveals that the phase transition from the zinc-blende structure to the rock-salt structure results from the distortion of tetrahedral angles and does not involve any bond breaking, in agreement with the MD simulations [7]. As pointed out in that study [7], these observations are in contrast to the transformation mechanism with the rhombohedral $R\bar{3}m$ intermediate state, which involves bond breaking. The simple

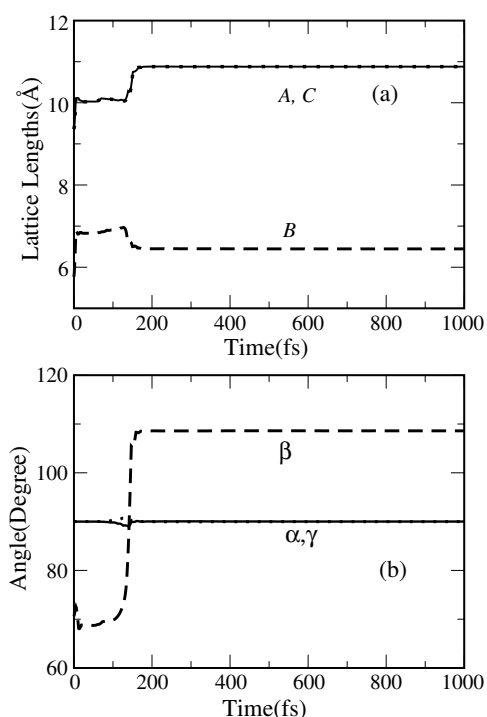


Figure 4. The simulation cell lengths and angles as a function of MD step at 0 GPa upon decompression.

transformation mechanism is illustrated in figure 3. For clarity, we show a small fragment of the simulation cell. During the transformation, the simulation cell length B ($\{010\}$ -direction in the zinc-blende structure) initially decreases to a small value while the other two perpendicular dimensions increase to a large value. Accompanied by this transformation, the Si and C atoms shift against each other along the compressed direction. This deformation produces some angular distortions in the system, and hence the bond angles differ substantially from the ideal tetrahedral angle (109.5°). For the tetragonal state, the bond angles become about 103° and 122° . As the monoclinic modification begins, we see a further closure and opening of the angles that gradually tend toward 90° and 180° , at which point the rock-salt structure is formed. As seen in the figure, the opening of the tetrahedron leads to channels for the neighbouring atoms to form a sixfold coordinated structure.

During the rock-salt to zinc-blende transformation, the deformation mechanism of the simulation cell is found to be different. In other words, the initial cubic simulation cell is not recovered and the transformation proceeds via a monoclinic to monoclinic modification of the simulation cell as seen in figure 4. Accompanied by the transformation, the β angle changes from 70° to 108° and the cell lengths A and C are dramatically elongated. The final monoclinic simulation box lengths A and C are about 21% longer than those of the initial cubic cell, while the B length is 27% shorter.

We find that the rock-salt to zinc-blende phase transition also involves both $I\bar{4}m2$ and $Imm2$ intermediate phases. However, several important distinctions relative to loading transition are observed during the transformation. The change from the rock-salt to orthorhombic phase is not dominantly caused by the angular distortion but by the elongation of the simulation cell lengths A and C . During this modification the β angle remains around 70° .

When the β angle is near 90° , the tetragonal $I\bar{4}m2$ phase is formed. Because of some distortion in the system, we are not able to identify clearly the space group of the structure when the β angle ranges from 94° to 103° . Above 103° , we observe the formation of the zinc-blende structure. The obtained lattice parameters and the coordinates of the transition states are summarized in table 1. These results are particularly important because they suggest that the zinc-blende to rock-salt and the rock-salt to zinc-blende phase transitions pass through the same intermediate states.

4. Conclusions

We have studied the pressure-induced phase transition of SiC with a constant-pressure *ab initio* technique. The method successfully produces the reversible phase transition between the zinc-blende and rock-salt structures. Moreover, the simulation provides detailed information regarding the nature of the transformation mechanism at the atomistic level. It is found that SiC undergoes a transition from the zinc-blende structure to the rock-salt structure through a tetragonal and an orthorhombic intermediate state. The space groups of the transition states are identified as $I\bar{4}m2$ and $Imm2$. Two important conclusions can be stated from the present simulation results. First, the $B3 \rightleftharpoons B1$ transition is based on a tetragonal $I\bar{4}m2$ and an orthorhombic $Imm2$ intermediate unstable state, and hence the transition cannot be described by an orthorhombic state alone. Second, the space group of the previously proposed orthorhombic intermediate state is actually $Imm2$ rather than $Pmm2$.

Acknowledgments

I am grateful to Dr D Hatch for fruitful discussions and Dr R Hundt for his valuable help in the use of the KPLOT program. I thank the SIESTA committee for providing the *ab initio* MD code and Dr Pablo Ordejón for helpful discussions about the dynamical simulation.

References

- [1] Addamino A 1974 *Silicon Carbide-1973* ed R C Marshall and J Faust Jr (Columbia: University of South Carolina Press) p 179
- [2] Strössner K and Cardona M 1987 *Solid State Commun.* **63** 113
- [3] Yosida M, Onodera A, Ueno M, Takemura K and Shimomura O 1993 *Phys. Rev. B* **48** 10587
- [4] Sekine T and Kobayashi T 1997 *Phys. Rev. B* **55** 8034
- [5] Chang K J and Cohen M L 1987 *Phys. Rev. B* **35** 8196
- [6] Karch K, Bechstedt F, Pavone P and Strauch D 1996 *Phys. Rev. B* **53** 13400
- [7] Shimojo F, Ebbsjö I, Lalia R, Nakano A, Rino J P and Vashista P 2000 *Phys. Rev. Lett.* **84** 3338
- [8] Catti M 2001 *Phys. Rev. Lett.* **87** 35504
- [9] Prez-Mato J M, Aroyo M, Capillas C, Blaha P and Schwarz K 2003 *Phys. Rev. Lett.* **90** 49603
- [10] Miao M S, Prikhodko M and Lambrecht W R L 2002 *Phys. Rev. B* **66** 64107
- [11] Miao M S, Prikhodko M and Lambrecht W R L 2002 *Phys. Rev. Lett.* **88** 189601
- [12] Miao M S and Lambrecht W R L 2003 *Phys. Rev. B* **68** 92103
- [13] Stokes H T and Hatch D 2002 *Phys. Rev. B* **65** 144114
- [14] Dong J, Hatch D, Stokes H T and Lewis J, unpublished
- [15] Ceperley D M and Alder M J 1980 *Phys. Rev. Lett.* **45** 566
- [16] Ordejón P, Artacho E and Soler J M 1996 *Phys. Rev. B* **53** 10441
Sánchez-Portal D, Ordejón P, Artacho E and Soler J M 1997 *Int. J. Quantum Chem.* **65** 453
- [17] Troullier N and Martins J L 1997 *Phys. Rev. B* **43** 1993
- [18] Parrinello M and Rahman A 1980 *Phys. Rev. Lett.* **45** 1196
- [19] Mizushima K, Yip S and Kaxiras E 1994 *Phys. Rev. B* **50** 14952
- [20] Durandurdu M and Drabold D A 2002 *Phys. Rev. B* **66** 045209
- [21] Hundt R, Schön J C, Hannemann A and Jansen M 1999 *J. Appl. Phys.* **32** 413